DR. JORGE MUSCHIETTI (Orcid ID : 0000-0002-5719-4833)

Article type : Research Letter

Arabidopsis pollen extensins LRX are required for cell wall integrity during pollen tube growth

Ana R. Sede [a,#], Cecilia Borassi [b,c#], Diego L. Wengier [a], Martín A. Mecchia [b], José M. Estevez [b,c*] and Jorge P. Muschietti [a,d*]

[a] Instituto de Investigaciones en Ingeniería Genética y Biología Molecular, "Dr. Héctor Torres" (INGEBI-CONICET), Vuelta de Obligado 2490, Buenos Aires, C1428ADN, Argentina

[b] Fundación Instituto Leloir, IIBBA-CONICET, Av. Patricias Argentinas 435, Buenos Aires, C1405BWE, Argentina

[c] Instituto de Fisiología, Biología Molecular y Neurociencias, IFIByNE-CONICET, Facultad de Ciencias Exactas y Naturales, Universidad de Buenos Aires, Int. Güiraldes 2160, Ciudad Universitaria, Buenos Aires, C1428EGA, Argentina

[d] Departamento de Biodiversidad y Biología Experimental, Facultad de Ciencias Exactas y Naturales, Universidad de Buenos Aires, Int. Güiraldes 2160, Ciudad Universitaria, Buenos Aires, C1428EGA, Argentina

[#]These authors equally contribute to this work

A.R.S and C.B. performed all the experiments, analyzed the data and wrote the paper. D.L.W. helped with some experiments. M.A.M. analyzed the data. J.P.M. and J.M.E. designed research, analyzed the data and supervised the project. A.R.S, D.L.W., J.P.M. and J.M.E. wrote the paper. All the authors have read the manuscript and have approved this submission.

This work was supported by grants from ANPCyT (PICT2013 and PICT2014 to JME; PICT2014 and PICT2015 to JPM).

*Correspondence to Corresponding authors: J.P.M. prometeo@dna.uba.ar and J.M.E. jestevez@leloir.com.ar

Abstract

Proper cell wall assembly is crucial during pollen tube growth. Leucine-rich repeat extensins (LRXs) are extracellular glycoproteins which belong to the hydroxyproline-rich glycoprotein (HRGP) family. They contain a conserved N-terminal leucine-rich repeat (LRR) domain and a highly variable C-terminal extensin domain. Here, we characterized four LRX proteins (LRX8 through LRX11) from pollen of *Arabidopsis thaliana*. To investigate the role of LRX8-LRX11 in pollen germination and pollen tube growth, multiple T-DNA *lrx* mutants were obtained. The *lrx* mutants display abnormal pollen tubes with an irregular deposition of callose and pectin. They also show serious alterations in pollen germination and segregation ratio. Our results suggest that LRXs are involved in ensuring proper cell wall assembly during pollen tube growth.

Keywords: cell wall, pollen tube, extensin, LRX, polarized growth, pectin, callose.

1. Introduction

Pollen tubes display polarized growth, a rapid and oscillatory mechanism that involves a tight coordination of reactive oxygen species (ROS), a Ca^{2+} gradient and a high traffic of vesicles to the pollen tube tip with a constant remodeling of the cell wall [1]. Mature pollen tube cell wall is composed by callose, non-esterified-pectins, glycoproteins and cellulose-like polymers deposited as sequential layers [2]. During polarized growth, cell wall must be rigid to withstand the internal turgor pressure but flexible enough to allow tip elongation. To this end, development of the growing tip cell wall must be strictly regulated by a proper assembly of a flexible network established by the crosslink of specific structural glycoproteins and methyl-esterified homogalacturonans within the extracellular matrix [3].

Pectin, the most abundant pollen cell wall component, is secreted at the pollen tube tip by exocytosis as a highly-methyl esterified polymer [4]. At the tip, de-esterification occurs by the activity of the PME (Pectin Methyl Esterase), that is regulated by PME-inhibitors specifically localized in this region [4]. Callose, a 1,3-β-D-glucan, is usually deposited at the cell wall reinforcing both compression and tension stresses [5]. Cellulose also has an important role in pollen tube growth, even though it is not a major constituent of the pollen tube cell wall. It has been reported that pollen tube growth is susceptible to cellulases [6] and to chemical inhibition of cellulose synthesis [7]. In agreement, cellulose synthase (CESAs) complexes were detected at the pollen tube tip [2, 8].

Leucine-rich repeat extensins (LRX) are proteins that contain a conserved N-terminal LRR domain and a typical C-terminal extensin domain with Ser-Pro$_{(3-5)}$ repetitive motifs possibly involved in crosslinking to cell wall components [9]. The LRR domain is highly conserved in monocots and dicots and potentially involved in ligand recognition and binding. Classical extensins are usually hydroxylated and then *O*-glycosylated on each hydroxyproline (Hyp) [9]. There are 11 LRX members in *Arabidopsis thaliana* separated in two large clades: LRX1-LRX7 belong to the vegetative clade and LRX8-LRX11 (originally known as PEX1-PEX4) to the reproductive clade [10-11]. In this work, we use the LRX8-LRX11 nomenclature to avoid confusions with the peroxin genes (named PEX) involved in peroxisome biogenesis [12].

The relationship between LRXs and polarized growth has been previously demonstrated. It has been shown that LRX1 and LRX2 are necessary for polar growth in root hair cells [10-11,13]. Two maize pollen extensins (mPex1 and mPex2) and one from tomato (tPex) have been characterized [14-16]. Even though expression profiling showed that Arabidopsis LRX8-LRX11 are highly expressed in pollen tubes (**Supplemental Figure 1A-B**), no function has been assigned to these proteins. Using genetic analyses, we showed that LRX8-11 are functionally redundant and required for pollen tube growth and maintaining cell wall integrity.

2. Materials and Methods

2.1. Plant material and growth conditions.

Arabidopsis thaliana ecotype Columbia-0 (Col-0) was used to perform all the experiments. Seeds were grown in soil and incubated at 22°C under constant light.

2.2. Identification of LRX T-DNA insertion lines.

T-DNA mutant lines were obtained from ABRC (Arabidopsis Biological Resource Center): for AT3G19020 (*LRX8*) we used salk_002743 (*lrx8-1*) and salk_031536 (*lrx8-2*). For AT1G49490 (*LRX9*), salk_137163 (*lrx9-1*) and salk_136163 (*lrx9-2*). For AT2G15880 (*LRX10*) salk_087083 *lrx10-1*), and for AT4G33970 (*LRX11*), salk_076356 (*lrx11-1*). Genotyping was performed as detailed on signal.salk.edu/tdnaprimers.2.html using the primers listed on **Table S1** and genomic DNA from rosette leaves.

2.3. *In silico* analyses.

LRX8-LRX11 protein sequences were used to build a phylogenetic tree using the Seaview 4.6.1 software [17]. LRX1 sequence was used as an out-group. Neighbor-joining tree was constructed based on the alignment of the complete amino acidic sequence of LRX8-LRX11 family members. The rooted tree represents a consensus tree generated by 1000 bootstrap replicates, each inferred from parametric distances by the neighbor-joining method [18]. Arabidopsis eFP Browser [19] was used for expression patterns of selected genes.

2.4. Gene expression analysis.

For RT-PCR analysis, mature pollen was germinated *in vitro* for 5 h and total RNA was isolated with RNeasy Plant Mini Kit (Qiagen) according to the manufacturer's instructions. cDNA was synthesized with M-MLV reverse transcriptase (Promega). PCR reactions were performed as follows: 4 min at 95°C, 34 cycles of 20 secs at 95°C, 30 sec at 57°C/60°C and 30 sec at 72°C. Actin was used as an internal standard. All primers used are listed in **Table S1**.

2.5. *In vitro* pollen germination.

One-day open flowers were collected and incubated for 30 min over a wet tissue in a wet chamber to allow pollen hydration. Anthers were dabbed on fresh semi-solid medium [20] to allow pollen grain release and pollen was incubated in a wet chamber at 22°C for 3 h. Images were captured in random fields using a bright-field Olympus BX41 microscope. Pollen germination analysis and pollen tube measurements were performed using ImageJ 1.51k software [21]. Values were reported as the mean ± SEM. For kinetics analysis, 7 pollen tubes from 2 independent lines (n=2) were measured every 10 min and growth rates were calculated.

2.6. Semi-*in vivo* and *in vivo* pollen germination.

One-day pre-emasculated pistils were hand-pollinated either with WT or mutant pollen. For semi-*in vivo* assays, styles were cut at the shoulder region of the ovary and positioned on semi-solid germination medium [22] at 22°C for 3 h. For *in vivo* assays, pistils were isolated 4 h after pollination and fixed with acetic acid:ethanol (1:3), rehydrated with an ethanol series (ethanol 70%, 50% and 30%) cleared with 8 M sodium hydroxide and stained with decolorized aniline blue [23]. Images were taken using an epifluorescence Olympus BX41 microscope under UV light with appropriate filter sets.

2.7. Pollen tube cell wall staining and imaging.

Pollen grains were germinated *in vitro* for 3 h on liquid germination medium [20] containing 0.15% agarose. Pectins were stained with propidium iodide (PI) (3 µM, final concentration). Callose was stained with Aniline Blue (AB) solution [23], by adding 5 µl AB to 20 µl of pollen-containing germination medium. Cellulose was stained with 0.01% Pontamine Fast Scarlet 4B (S4B) [24]. In all cases, fluorescence along the cell wall encompassing the pollen tube tip and subapical region was determined using the segmented line function in ImageJ 1.51k (with a line width of 15). The integrated fluorescence was normalized to the perimeter of the measured region. This strategy allows for direct comparison between pollen tubes of different width. PI and S4B measurements were determined on confocal sections obtained with Leica SPE and Zeiss Meta 510 LSM confocal microscopes. Callose images were taken using an epifluorescence Olympus BX41 microscope under UV light.

ROS quantification of pollen tubes growing *in vitro* were performed by incubating the samples with 25 µM H_2DCFDA (Sigma) for 5 min and images were taken as was described above.

3. Results

3.1. Double and triple mutants for pollen *LRX* show deficiencies in pollen tube cell wall integrity

According to available pollen transcriptomic data (http://genevestigator.com/gv ; [25]), all *LRX* genes are highly expressed in mature pollen and pollen tubes (**Supplemental Figure 1A-B**). Structurally, LRX8-LRX11 have a conserved N-terminal domain containing 11 repetitions of the LRR motif followed by a cysteine rich domain and a highly variable C-terminal extensin domain with 14 up to 25 Ser-$Pro_{(3-5)}$ repetitions (**Figure 1A**). All of them display a putative signal peptide (SP) that could be necessary for export to the pollen cell wall. Based on protein sequence homology, LRX8-LRX9 and LRX10-LRX11 cluster together in two homologous groups (**Supplemental Figure 1C**). In order to study the function of the LRXs in pollen germination and pollen tube growth, T-DNA insertional mutant lines were obtained for all the pollen LRXs (**Figure 1A**). Transcript levels in homozygous lines were analyzed by RT-PCR using total RNA from germinated pollen. **Figure 1B** shows null expression of the corresponding *LRX* genes in all single mutant lines analyzed except for *lrx8-1*. This line was discarded for future analysis.

To investigate the role of LRXs during pollen germination and pollen tube growth, WT and mutant *lrx* pollen were germinated *in vitro* (**Figure 2**). A statistically significant reduction in pollen germination was observed for all mutants, except for *lrx8-2*. Considering the high amino acidic identity among the LRR domain of the different LRXs and the fact that all LRXs are highly and preferentially expressed in pollen, functional redundancy was expected. To determine if successive elimination of LRXs resulted in more severe phenotypes, several double (*lrx8-2 lrx10-1, lrx9-2 lrx10-1, lrx9-2 lrx11-1* and *lrx8-2 lrx11-1*) and one triple (*lrx9-2 lrx10-1 lrx11-1)* homozygous mutant were obtained. As expected, double mutants showed a statistically significant reduction in pollen germination. Furthermore, the triple mutant

lrx9-2 lrx10-1 lrx11-1 showed a reduction of germination to 39.3% when compared to WT pollen (**Figure 2A**). Next, we evaluated pollen tube growth for WT and *lrx* mutants. Because aberrant pollen tubes were detected in mutant backgrounds (see below), pollen tube length was measured by selecting healthy mutant pollen tubes excluding those that showed abnormal phenotypes. No significant differences in pollen tube length were found between WT and mutant pollen tubes germinated *in vitro* for 3 h, except for *lrx8-2 lrx10-1* double mutant that showed slightly longer tubes (**Supplementary Figure 2**).

Many abnormal pollen tubes were observed for all double and the triple mutant *lrx9-2 lrx10-1 lrx11-1* when compared to WT and to all single *lrx* mutants after 3 h of *in vitro* germination (**Figure 2B**). These abnormalities include wavy growth, widened tips or the emergence of a bulge at the shank or at the pollen tube tip which causes tip bursting (**Figure 2C**). Moreover, after 8 h of *in vitro* growth, 94% of the triple mutant *lrx9-2 lrx10-1 lrx11-1* pollen tubes showed abnormal phenotypes confirming the relevance of the LRX proteins during pollen tube growth and suggesting that *lrx* mutants show a progressive degeneration of pollen tubes. Therefore, pollen tube growth rate was analyzed. Kinetic analysis of *in vitro* growing abnormal pollen tubes showed that after an initial normal growth (0-60 min), the triple mutant *lrx9-2 lrx10-1 lrx11-1* growth rate (181.5 µm/h) was lower than WT (214.0 µm/h) (**Figure 3A**). Time-lapse imaging of a representative pollen tube shows that after 60 min the tube stopped growing and a big bulge appeared at the subapical region (see asterisks in **Figure 3B**).

LRXs are predicted to be active at the cell wall thus aberrant pollen tubes and tip bursting in the mutants could be explained by changes in the cell wall composition. Based on this hypothesis, cell wall components of WT and triple mutant *lrx9-2 lrx10-1 lrx11-1* in *in vitro* germinated pollen tubes were stained with different dyes (**Figure 4 A-C-D**). We used propidium iodide (PI) which stains pectin trough the binding to the carboxyl residues on non-methoxylated homogalacturonans of pectins [26], aniline blue (AB) which stains callose [27] and Pontamine Fast Scarlet 4B (S4B) for cellulose detection [24]. Triple mutant *lrx9-2 lrx10-1 lrx11-1* pollen tubes showed an abnormal accumulation of pectin and callose where the bulge appears (**Figure 4A-C**). We also observed that while pectins appear to be present in the bulge (**Figure**

4A), callose aberrantly accumulates at the point of emergence (**Figure 4C**). When the PI, AB and S4B signals were quantified along the cell wall of the pollen tubes from the tip to the subapical area (**Figures 4A-C-D**), significant differences were found in pectin and callose content. When a transverse line through the subapical region of pollen tubes stained with PI was used, we found that in the triple mutant *lrx9-2 lrx10-1 lrx11-1* the signal at the margins of the tubes was several times brighter than in WT tubes (**Figure 4B**). All these results suggest that the lack of pollen LRXs produces abnormal cell walls (with altered levels of pectin/callose components) with a failure in their structural integrity causing a complete shutdown of the polar growth and the focal breakdown of the cell wall at the apical or subapical regions of pollen tubes.

Finally, since ROS is required for normal pollen tube growth [28], 2,7-dichlorofluorescein diacetate probe (H_2DCF-DA) was used to analyze ROS levels in triple mutant pollen tubes, but no significant differences were found compared to the WT (**Supplementary Figure 3**). Further analyses using ROS biosensors (e.g. Hyper) will be required to explore with more detail whether ROS homeostasis is altered during the bulge formation in the triple mutant *lrx9-2 lrx10-1 lrx11-1*.

3.2. Triple *lrx9-2 lrx10-1 lrx11-1* mutant shows defects in fertilization and seed development

To test whether abnormal pollen tube growth has a direct impact on male pollen transmission and competitiveness *in vivo*, we analyzed the segregation of self-crosses of heterozygous double and the triple *lrx* mutants. A skewed segregation ratio compatible with defects in pollen transmission was observed in progenies of double *lrx* mutants (**Table 1**). The highly-distorted ratio obtained for the double mutants *lrx8-2 lrx10-1* (1:100.3) and *lrx8-2 lrx11-1* (1:115) and the fact that no triple mutant *lrx8-2 lrx9-2 lrx10-1* was obtained after analyzing 115 plants when mutant plants *lrx8-2*$^{+/-}$ *lrx9-2*$^{+/-}$ *lrx10-1*$^{-/-}$ were self-crossed, suggest that even though LRX8 and LRX10 or LRX11 belong to different subclades of pollen LRX's family (**Supplemental Figure 1C**), they are required to be present simultaneously. This also could explain why we did not obtain the quadruple *lrx* mutant.

The physiological significance of eliminating LRXs was further addressed in semi-*in vivo* and *in vivo* pollination assays. When pollen of the triple mutant *lrx9-2 lrx10-1 lrx11-1* was used (**Figure 5A-B**, middle panel) to pollinate WT stigmas, most of the tubes displayed expanded tips when compared with pollinations where WT pollen was used (**Figure 5A-B**, left and right panels). When tested *in vivo*, most of the triple mutant *lrx9-2 lrx10-1 lrx11-1* pollen tubes arrest their growth within the pistil showing expanded tips (**Figure 5C**). Furthermore, triple mutant *lrx9-2 lrx10-1 lrx11*-1 showed a reduction by 67% in seed set per silique when compared to the WT (**Figure 5D**). Altogether, these results suggest that defects in fertilization and seed development of the triple mutant *lrx9-2 lrx10-1 lrx11-1* are caused by the abnormal pollen tube cell wall integrity.

4. Discussion

Our results show that pollen LRXs are functionally redundant regulating proper pollen tube growth. In the absence of LRXs, cell wall assembly is severely affected with an increased accumulation of callose and pectin resulting in abnormal pollen tubes that develop bulges and burst. Our work confirms previous findings where LRX are necessary for appropriate cell wall development [11,13]. The changes observed in the triple mutant *lrx9-2 lrx10-1 lrx11-1* seem to underlie a structural defect of the pollen tube cell wall.

Functional studies of proteins containing EXT domains suggest that their Tyr residues are intra/intercross-linked to build a three-dimensional linkage that interacts with the pectin network [29], supporting a structural role of LRXs. Furthermore, it was reported that LRX1 plays an important structural role as a glycoprotein physically linked to the cell wall and required to maintain a normal polar-growth in root hair cells [11,13]. *lrx1* mutant showed swollen root hairs that eventually burst in a similar manner than the triple pollen *lrx9-2 lrx10-1 lrx11-1* mutant. Interestingly, *lrx1* phenotype could be rescued by *ROL1* (for repressor of *lrx1*) gene allelic to *RHM1* (for RHaMnose biosynthesis 1), which is involved in the formation of UDP-L-Rha, a building block of the pectin backbones in rhamnogalacturonan I (RG-I) and rhamnogalacturonan II (RG-II) [30]. As expected, *ROL1* suppressor mutations (*rol1-1*

and *rol1-2*) modify the pectic polysaccharide RG-I and RG-II suggesting again a close relationship between EXT-like proteins and the pectin network. It would be interesting to test whether *ROL1* mutations or any pectin-related mutant that change the levels of RG-I/RG-II cell wall components can also suppress the triple *lrx* mutant pollen phenotype. The main difference between the pollen LRX8-LRX11 and the root hair LRX1 is the level of functional redundancy probably linked to the strong selection found in gametophytic pollen. Therefore, pollen tubes may have developed more robust mechanisms to control cellular integrity by increasing gene duplication events leading to more frequent functional redundancy (e.g. RBOHJ/RBOHH two NADPH oxidases for ROS-production [31], ANXR1/ANXR2, two pollen-specific receptor kinases as extracellular sensors [32], multiple GLR channels for Ca^{2+} signaling [33], etc.). In this context, it seems that the lack of LRX8-LRX11 proteins triggered detectable changes in the cell walls of pollen tubes such as callose and pectin over-accumulation. On the other hand, normal levels of cellulose are not sufficient to maintain the structural integrity of the cell walls. Although both, pollen tubes and root hair cells, display polarized growth toward several external cues, differences in the build-up of nascent cell walls at the apical dome would explain why pollen tubes elongate at much higher rates (up to 1 μm sec^{-1}) than root hair cells (up to 1 μm min^{-1}) [2, 34]. Based on this, pollen tubes respond to deficient cell wall deposition faster than root hairs.

The lack of LRX8-LRX11 proteins causes a phenotype resembling previous reported for other proteins required for normal pollen tube growth. For example, pollen overexpressing RAC/ROPs (for RAC-like/RHOs of plants) show a balloon-shaped tube and growth arrest [35]. In addition, down-regulation of RAC/ROP affects the elongation rate and tip growth resulting in wider pollen tubes. This phenotype of depolarized pollen tube growth is observed when the pathway of actin depolymerization factor is affected [35]. Similarly, the overexpression of the tomato pollen-specific LRR-receptor kinases, LePRK1 and LePRK2, led to a permanent formation of blebs at the tip [36] and swollen tips [37] respectively, probably due to the lack of polarity. The cytoplasmic domains of LePRK1 and LePRK2 interact with KPP (Kinase Partner Protein) [38], a tomato pollen ROP-GEF that activates ROP *in vitro* [39]. Pollen tubes overexpressing KPP showed ballooned tips and irregular actin deposition and cytoplasmic streaming as observed by up-regulating RAC/ROP

signaling [36]. Similar *in vitro* pollen tube bursting phenotypes have been also reported in Arabidopsis for the double mutants *anxur1*/*anxur2* (*anx1*/*anx2*) [40] and *rbohH*/*rbohJ* NADPH oxidases [31] and for the single mutant *vanguard* (*vgd1*) [41]. ANXUR1 and ANXUR2 activate ROP and then RbohH and RbohJ, modulating ROS production and synthesis of new cell wall precursors [31]. VANGUARD (VGD1) is a pollen PME-like protein that would control the demethylesterification of the linear homopolymer (1,4)-linked-α-D-galacturonic acid homogalaturonan (HGA), a pectic polysaccharide of the cell wall [41]. When exogenous PME was added to the pollen germination media, there is an increase in the thickening of the cell wall at the tip and concertedly growth is inhibited [4]. This suggests that an increase in pectin demethoxylated HG is enough to affect pollen tube growth.

The role of the LRR domain in the N-terminus of LRXs is less predictable than the EXT domain. The LRR domain could be interacting with specific pollen or pistil ligands. LRXs localization is compatible with this hypothesis since a maize LRX protein was immunohistochemically localized at the intine layer in mature pollen [15]. Moreover, a yeast two-hybrid screen using the LRR domain of tomato pollen-specific LRX as bait, identified a pollen specific RAPID ALKALINIZATION FACTOR (SlPRALF) [42]. The extracellular localization of SlPRALF, confirmed by the identification of the processed SlPRALF peptide in pollen germination media [42], suggests that the interaction between RALF-LRX occurs in the pollen cell wall-membrane continuum. If LRXs act as RALF ligand in Arabidopsis pollen and what kind of response this interaction triggers remain to be determined. Further deep biochemical studies in isolated pollen tube cell walls are required to address the exact nature of these cell wall changes and how they compromise their integrity during active growth.

5. Conclusion

Our results suggest that pollen LRXs play a role in the maintenance of cell wall integrity and prevent bursting during pollen germination and pollen tube growth. A proposed model is that during pollen tube growth, LRXs are exported to the pollen cell wall-membrane continuum to monitor the condition of the cell wall. Through an

LRR domain-mediated interaction with a putative pollen or pistil ligand or with a domain of a pollen membrane-intrinsic protein, successive activation of the RLK-ROP signaling module, vesicle secretion to the tube tip and maintenance of cell wall integrity are sustained. This highlights that a complex through an obscure interlaced pathway may exist between LRXs, ligands, RLKs and apical dome components (ROP-actin) in the pollen tube cytoplasm directing the deposition of new cell wall material during pollen tube growth.

Acknowledgments

We thank the Arabidopsis Biological Resource Center (ABRC) at Ohio State University and the NASC-European Arabidopsis Stock Centre for providing the T-DNA insertion lines. No conflict of interest declared. This work was supported by grants from ANPCyT (PICT2013-003 and PICT2014-504), and ICGEB2016 to J.M.E. and PICT2014-0423 and PICT2015-0078 to J.P.M.

Supplemental data

The following supplemental materials are available.

Supplementary Figure 1 (**A**) Expression patterns of *LRX8-LRX11* in different Arabidopsis tissues based on Genevestigator. (**B**) Arabidopsis eFP Browser analysis of LRX8-LRX11. (**C**) Phylogenetic tree of Arabidopsis pollen LRX. Phylogenetic analysis was done using Seaview 4.6.1 software and the protein sequence neighbor-joining method. LRX1 was used as an out-group.

Supplementary Figure 2 Pollen tube length of simple, double and the triple *lrx* mutants after 3 h of incubation. Data are shown as the mean ± SEM for *lrx8-2* (n=6), for *lrx9-2* (n=5), *lrx10-1* (n=3), *lrx11-1* (n=11), *lrx8-2 lrx10-1* (n=11), *lrx9-2 lrx11-1* (n=6), *lrx9-2 lrxlrx10-1* (n=10) and *lrx9-2 lrx10-1 lrx11-1* (n=13). Independent plants with more than 80 pollen grains were analyzed per genotype and experiment. Mean values were normalized to Col-0 set as 100 % of length. Asterisks represent significant differences form Col-0 according to one-way ANOVA test (*) $p \leq 0.05$.

Supplementary Figure 3 Quantification and representative images of ROS levels in pollen tubes stained with H_2DCFDA. Scale bar: 10 µm.

Table S1. Primer list used in this study.

Cross	Segregation Genotype	Expected ratio	Observed ratio	X^2 p value
lrx9-2$^{+/-}$ *lrx11-1*$^{+/-}$ x self	Double homozygous	1:16	3:92	ns
lrx8-2$^{+/-}$ *lrx10-1*$^{+/-}$ x self	Double homozygous	1:16	3:301	p<0.05
lrx8-2$^{+/-}$ *lrx11-1*$^{+/-}$ x self	Double homozygous	1:16	1:115	p<0.05
lrx9-2$^{+/-}$ *lrx10-1*$^{+/-}$ x self	Double homozygous	1:16	3:133	ns
lrx10-1$^{+/-}$ *lrx11-1*$^{+/-}$ x self	Double homozygous	1:16	1:100	p<0.05
lrx8-2$^{+/-}$ *lrx9-2*$^{+/-}$ *lrx10-1*$^{-/-}$ x self	Triple homozygous	1:16	0:115	ND
lrx9-2$^{-/-}$ *lrx10-1*$^{+/-}$ *lrx11-1*$^{+/-}$ x self	Triple homozygous	1:16	7:174	ns

Table 1. **Disruption of *LRX8-LRX11* genes causes defective male-specific gene transmission.** Segregation analysis of double and triple *lrx* T-DNA mutants. ns= not significant. ND: not determined. For all cases mutants genotyping was carried out by PCR using the primers listed in **Table S1**.

Figure Legends

Figure 1 (**A**) Schematic representation of LRX8-LRX11 proteins showing domain organization and T-DNA insertional sites. Introns (curved line in LRX10), exons (rectangles), 5'UTR (yellow square in LRX8), LRR domain (grey), extensin domain (red) and positions of T-DNA insertions are indicated. Prom: promoter region in LRX8**.** (**B**) Validation of single *lrx* T-DNA mutant lines. Total RNA was extracted from *in vitro* germinated pollen tubes. Actin 8 (*ACT8*) was used as a control. The primers used for RT-PCR are listed in **Table S1**.

Figure 2 (**A**) Pollen germination rates of single, double and triple *lrx* mutants. Data are shown as the mean ± SEM for *lrx8-2* (n=3), for *lrx9-2* (n=3), for *lrx10-1* (n=8), for *lrx11-1* (n=7), for *lrx8-2 lrx10-1* (n=11), for *lrx9-2 lrx11-1* (n=6), for *lrx9-2 lrx10-1*

(n=3) and for *lrx9-2 lrx10-1 lrx11-1* (n=15) where "n" corresponds to the number of independent plants with more than 80 pollen grains analyzed per genotype and experiment. Mean values were normalized to Col-0 (n=10) that was set at 100% of germination. Asterisks represent significant differences from Col-0 according to a Student's *t* test: (*) $p \leq 0.05$, (**) $p \leq 0.01$ and (***) $p \leq 0.001$. (**B**) Percentage of abnormal pollen tubes over total germinated pollen for simple, double and the triple mutant *lrx9-2 lrx10-1 lrx11-1* after 3 h of germination. Data are shown as the mean ± SEM for Col-0 (n=33), for *lrx8-2* (n=3), for *lrx9-2* (n=4), for *lrx10-1* (n=8), for *lrx11-1* (n=7), for *lrx8-2 lrx10-1* (n=7), for *lrx9-2 lrx11-1* (n=6), for *lrx9-2 lrx10-1* (n=3) and for *lrx9-2 lrx10-1 lrx11-1* (n=15) where "n" corresponds to the number of independent plants with more than 80 pollen grains analyzed per genotype and experiment. Asterisks indicate significant differences from Col-0 according to a one-way ANOVA test: (***) $p \leq 0.001$. (**C**) Representative DIC images of WT and *lrx9-2 lrx10-1 lrx11-1* pollen tubes. Scale bar: 10 µm.

Figure 3 (**A**) Kinetic analysis of *in vitro* growing of Col-0 and triple mutant *lrx9-2 lrx10-1 lrx11-1* pollen tubes. Data are shown as the mean ± SEM of two independent experiments with 7 pollen tubes analyzed per experiment. Asterisks indicate significant differences from Col-0 according to Student's *t* test (*) $p \leq 0.05$, (**) $p \leq 0.01$ and (***) $p \leq 0.001$. (**B**) *In vitro* growing time-lapse image of a representative abnormal pollen tube of the triple mutant *lrx9-2 lrx10-1 lrx11-1*. Asterisks indicate where a bulge is formed. Scale bar=100 µm. Pollen tubes stop growing before forming the bulges at the tip and frequently burst.

Figure 4 Quantification of cell wall components in Col-0 and triple mutant *lrx9-2 lrx10-1 lrx11-1* pollen tubes. Representative images of pollen tubes stained with propidium iodide (PI) (**A-B**), aniline blue (AB) (**C**) and Pontamine Fast Scarlet 4B (S4B) (**D**)**.** Asterisks indicate significant differences from Col-0 according to Student's *t* test (*) $p \leq 0.05$. Scale bar: 5 µm (**A**); 10 µm (**C-D**). For PI (**A**), AB (**C**) and S4B (**D**) quantifications, a signal along the cell wall of the pollen tubes from the tip to the subapical area was obtained. The fluorescent signal was normalized to the pollen

tube perimeter of the measured region. For (**B**), a transversal line at 5 µm away from the tip was defined. Triple mutant measurements were performed including all pollen tubes despite their degree of abnormality; the bulge was always excluded from the measurements.

Figure 5 (**A**) Representative images of WT (left and right panel) and triple mutant *lrx9-2 lrx10-1 lrx11-1* (middle panel) pollen tubes growing through WT (left and middle panels) or triple mutant *lrx9-2 lrx10-1 lrx11-1* (right panel) pistils in a semi *in vivo* assay. Styles were observed 3h after hand pollination. Arrowheads indicate abnormal pollen tubes found only in mutant pollen. Scale bar: 200 µm. (**B**) Semi-*in vivo* assays quantification. Data are shown as the mean ± SEM of 13 and 8 pollinations for WT and the triple mutant *lrx9-2 lrx10-1 lrx11-1*, respectively. (**C**) Representative images of aniline blue staining of *in vivo* WT (left panel) and triple mutant *lrx9-2 lrx10-1 lrx11-1* (middle panel) growing pollen tubes 4 h after hand self-pollination. Right panel shows an inset of the middle image as indicated. Arrowheads indicate abnormal pollen tubes. Scale bars: left and middle panel: 100 µm, right panel: 50 µm. (**D**) Number of seeds per silique in WT and triple mutant *lrx9-2 lrx10-1 lrx11-1* plants. Data are shown as the mean ± SEM of 11 independent plants with 10 siliques analyzed for each plant. Asterisks indicate significant differences from Col-0 according to a Student's *t* test with (***) $p \leq 0.001$. Arrowheads indicate unfertilized or aborted ovules.

LITERATURE CITED

[1] Cheung A.Y. and Wu H.M. (2008). Structural and signaling networks for the polar cell growth machinery in pollen tubes. *Annu. Rev. Plant Biol*. 59:547–72.

[2] Chebli Y., Kaneda M., Zerzour R., and Geitmann A. (2012). The Cell Wall of the Arabidopsis Pollen Tube—Spatial Distribution, Recycling, and Network Formation of Polysaccharides. *Plant Physiology* 160 (4): 1940-1955.

[3] Hepler P.K., Rounds C.M., Winship L.J. (2013). Control of cell wall extensibility during pollen tube growth. *Molecular Plant* 6: 998-1017.

[4] Bosch M, Cheung AY, Hepler PK (2005). Pectin methylesterase, a regulator of pollen tube growth. Plant Physiol 138: 1334–1346.

[5] Parre E, Geitmann A. (2005). More than a leak sealant. The mechanical properties of callose in pollen tubes. Plant Physiol 137: 274–286

[6] Aouar, L., Chebli, Y., and Geitmann, A. (2010). Morphogenesis of complex plant cell shapes: the mechanical role of crystalline cellulose in growing pollen tubes. *Sex. Plant Reprod*. 23, 15–27.

[7] Anderson, J.R., Barnes, W.S., and Bedinger, P. (2002). 2,6-dichlorobenzonitrile, a cellulose biosynthesis inhibitor, affects morphology and structural integrity of petunia and lily pollen tubes. *J. Plant Physiol*. 159, 61–67.

[8] Cai, G., Faleri, C., Del Casino, C., Emons, A.M.C., and Cresti, M. (2011). Distribution of callose synthase, cellulose synthase, and sucrose synthase in tobacco pollen tube is controlled in dissimilar ways by actin filaments and microtubules. *Plant Physiol*. 155, 1169–1190.

[9] Borassi C., Sede A.S., Mecchia, M., Muschietti J.P., and Estevez J.M. (2015). An update on cell surface proteins containing extensin-motifs. *J. Exp. Bot.* 76(2): 477-487*.*

[10] Ringli C. (2010). The hydroxyproline-rich glycoprotein domain of the Arabidopsis LRX1 requires Tyr for function but not for insolubilization in the cell wall. *The Plant Journal* 63, 662–669.

[11] Baumberger N., Steiner M., Ryser U., Keller B. and Ringli C. (2003). Synergistic interaction of the two paralogous Arabidopsis genes LRX1 and LRX2 in cell wall formation during root hair development. *The Plant Journal* 35, 71–81.

[12] Nito K., Kamigaki A., Kondo M., Hayashi M. and Nishimura M. (2007). Functional classification of Arabidopsis peroxisome biogenesis factors proposed from analyses of knockdown mutants. *Plant Cell Physiol*. 48(6):763-74.

[13] Baumberger N., Ringli C. and Keller B. (2001). The chimeric leucine rich repeat/extensin cell wall protein LRX1 is required for root hair morphogenesis in Arabidopsis thaliana. *Genes & Development* 15, 1128–1139.

[14] Rubinstein A. L., Broadwater A. H., Lowrey K. B. and Bedinger P. A. (1995a) *Pex1*, a pollen-specific gene with an extensin-like domain. *Proc. Natl. Acad. Sci.* 92, 3086-3090.

[15] Rubinstein A. L., Márquez J., Suárez-Cervera M. and Bedinger P. A. (1995b) Extensin-like glycoproteins in the maize pollen tube wall. *The Plant Cell*. 7: 2211-2225.

[16] Stratford S., Barne W., Hohorst D.L., Sagert J.G., Cotter R., Golubiewski A., Showalter A.M., McCormick S., and Bedinger P. (2001). A leucine-rich repeat region is conserved in pollen extensin-like (Pex) proteins in monocots and dicots. *Plant. Mol. Biol*. 46: 43-56.

[17] Gouy, M. Guindon, S. & Gascuel., O. (2010). SeaView version 4: a multiplatform graphical user interface for sequence alignment and phylogenetic tree building. *Molecular Biology and Evolution.* 27(2):221-224.

[18] Saitou N. and Nei M. (1987). The neighbor-joining method: a new method for reconstructing phylogenetic trees. *Molecular biology and evolution* 4, 406–425.

[19] Winter D., Vinegar B., Nahal H., Ammar R., Wilson G.V., and Provart N.J. (2007). An "Electronic Fluorescent Pictograph" Browser for Exploring and Analyzing Large-Scale Biological Data Sets. *PLOS ONE* 2(8): e718. doi: 10.1371/journal.pone.0000718.

[20] Boavida L.C. and McCormick S. (2007). Temperature as a determinant factor for increased and reproducible *in vitro* pollen germination in Arabidopsis thaliana. *The Plant Journal* 52, 570–582.

[21] Schindelin, J.; Arganda-Carreras, I., Frise, E., Kaynig V., Longair M., Pietzsch T., Preibisch S., Rueden C., Saalfeld S., Schmid B., Tinevez JY., White D.J., Hartenstein V., Eliceiri K., Tomancak P. and Cardona A. (2012), Fiji: an open-source platform for biological-image analysis. *Nature methods* 9(7): 676-682.

[22] Palanivelu R. and Preuss D. (2006). Distinct short-range ovule signals attract or repel *Arabidopsis thaliana* pollen tubes in vitro. BMC *Plant Biol.* 6, 7.

[23] Mori T., Kuroiwa H., Higashiyama T., and Kuroiwa T. (2006). GENERATIVE CELL SPECIFIC 1 is essential for angiosperm fertilization. *Nature Cell Biology* 8, 64–71.

[24] Anderson C. T, Carroll A., Akhmetova L., and Somerville C. (2010) Real-Time Imaging of Cellulose Reorientation during Cell Wall Expansion in Arabidopsis Roots. *Plant Physiol.* 152: 787–796.

[25] Loraine A.E., McCormick S., Estrada A., Patel K., and Qin P. (2013). RNA-Seq of Arabidopsis pollen uncovers novel Transcription and alternative splicing. *Plant Physiology* 162: 1092-1109.

[26] Rounds, C.M., Lubeck, E., Hepler, P.K. and Winship, L.J. (2011) Propidium iodide competes with Ca^{2+} to label pectin in pollen tubes and Arabidopsis root hairs. *Plant Physiology* 157, 175–187.

[27] Ischebeck T., Stenzel I., Heilmann I. (2008). Type B phosphatidylinositol-4-Phosphate 5-kinases mediate Arabidopsis and *Nicotiana tabacum* pollen tube growth by regulating apical pectin secretion. *The Plant Cell* 20: 3312-3330.

[28] Wudick M.M. and Feijó J.A. (2014). At the intersection: merging Ca2+ and ROS signaling pathways in pollen. *Mol. Plant.* 7(11):1595-7. doi: 10.1093/mp/ssu096.

[29] Cannon M.C., Terneus K., Hall Q., Tan L., Wang Y., Wegenhart B.L., Chen L., Lamport D.T., Chen Y., and Kieliszewski M.J. (2008). Self-assembly of the

plant cell wall requires an extensin scaffold. *Proc. Natl. Acad. Sci.* 105, 2226–2231.

[30] Diet A., Link B., Seifert G., Schellenberg B., Wagner U., Pauly M., Reiter WD., and Ringli C. (2006). The Arabidopsis Root Hair Cell Wall Formation Mutant lrx1Is Suppressed by Mutations in the RHM1 Gene Encoding a UDP-L-Rhamnose Synthase. *The Plant Cell* 18: 1630-1641.

[31] Kaya H., Iwano M., Takeda S., Kanaoka MM., Kimura S., Abe M., and Kuchitsu K. (2015). Apoplastic ROS production upon pollination by RbohH and RbohJ in Arabidopsis. *Plant Signal Behav.* 10(2): e989050.

[32] Boisson-Dernier A., Lituiev D., Nestorova A., Franck C.M., Thirugnanarajah S., and Grossniklaus U. (2013). ANXUR Receptor-Like Kinases Coordinate Cell Wall Integrity with Growth at the Pollen Tube Tip Via NADPH Oxidases. *PLoS Biol*. 11(11):e1001719.

[33] Michard E., Lima P., Borges F., Silva A.C., Portes M.T., Carvalho J.E., Giliham M., Liu L., Obermeyer G., and Feijó JA. (2011). Glutamate receptor–like genes form Ca2+ channels in pollen tubes and are regulated by pistil D-Serine. *Science* 332(6028): 434-7.

[34] Grierson, C., Nielsen, E., Ketelaarc, T. and Schiefelbein, J. (2014) Root Hairs. *The Arabidopsis Book/American Society of Plant Biologists.* **12**, e0172.

[35] Zou Y., Aggarwal M., Zheng W.G., Wu H.M., and Cheung AY. (2011). Receptor-like kinases as surface regulators for RAC/ROP-mediated pollen tube growth and interaction with the pistil. *AoB Plants*. plr017.

[36] Gui C., Dong X., Liu H., Huang W., Zhang D., Wang S., Barberini ML., Gao X., Muschietti J., McCormick S., and Tang W. (2014). Overexpression of the tomato pollen receptor kinase LePRK1 rewires pollen tube growth to a blebbing mode. *The Plant Cell* 26: 3538-55.

[37] Salem T., Mazzella A., Barberini M.L., Wengier D., Motillo V., Parisi G., and Muschietti J. (2011). Mutations in Two Putative Phosphorylation Motifs in the Tomato Pollen Receptor Kinase LePRK2 Show Antagonistic Effects on Pollen Tube Length. *The Journal of Biological Chemistry* 286, 4882–4891.

[38] Kaothien P., Ok S.H., Shuai B., Wengier D., Cotter R., Kelley D., Kiriakopolos S., Muschietti J., and McCormick S. (2005) Kinase partner protein interacts with the LePRK1 and LePRK2 receptor kinases and plays a role in polarized pollen tube growth. *The Plant Journal* 42, 492-503.

[39] Löcke S., Fricke I., Mucha E., Humpert M.L., and Berken A. (2010). Interactions in the pollen-specific receptor-like kinases-containing signaling network. *Eur. J Cell Biol*. 89: 917-23.

[40] Boisson-Dernier A., Roy S, Kritsas K., Grobei MA., Jaciubek M., Schroeder JI., Grossniklaus U. (2009). Disruption of the pollen-expressed FERONIA homologs ANXUR1 and ANXUR2 triggers pollen tube discharge. *Development.* 136(19):3279-88.

[41] Jiang L., Yang SL., Xie LF., Puah CS., Zhang XQ., Yang WC., Sundaresan V. and Ye D. (2005). VANGUARD1 Encodes a Pectin Methylesterase That Enhances Pollen Tube Growth in the Arabidopsis Style and Transmitting Tract. *Plant Cell.* 17(2): 584–596.

[42] Covey PA., Subbaiah CC., Parsons RL., Pearce G., Lay FT., Anderson MA., Ryan CA. and Bedinger PA. (2010). A Pollen-Specific RALF from Tomato That Regulates Pollen Tube Elongation. *Plant Physiol*. 153(2): 703–715.

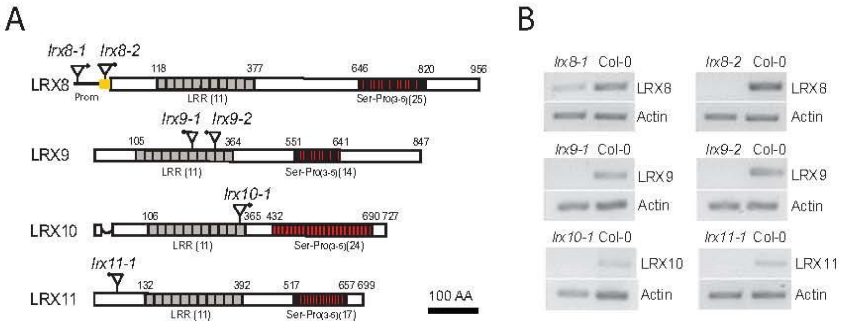

Figure 1 (A) Schematic amino acidic representation of LRX8-LRX11 proteins showing domain organization and T-DNA insertional sites. Introns (curved line), exons (rectangles), 5'UTR (yellow square), LRR domain (grey), EXT domain (red) and positions of T-DNA insertions are indicated. Prom: promoter region. (B) Validation of single *lrx* T-DNA mutant lines. Total RNA was extracted from *in vitro* germinated pollen tubes. Actin 8 (ACT8) was used as a control. The primers used for RT-PCR are listed in Table S1.

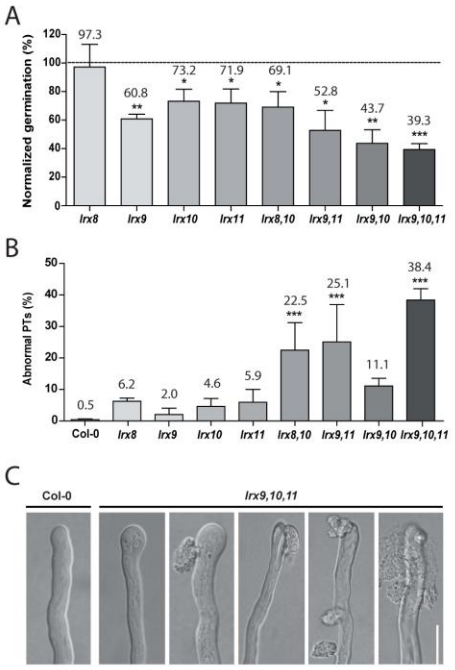

Figure 2 (A) Pollen germination rates of single, double and triple *lrx* mutants. Data are shown as the mean ± SEM for *lrx8-2* (n=3), for *lrx9-2* (n=3), for *lrx10-1* (n=8), for *lrx11-1* (n=7), for *lrx8-2 lrx10-1* (n=11), for *lrx9-2 lrx11-1* (n=6), for *lrx9-2 lrx10-1* (n=3) and for *lrx9-2 lrx10-1 lrx11-1* (n=15) where "n" corresponds to the number of independent plants with more than 80 pollen grains analyzed per genotype and experiment. Mean values were normalized to Col-0 (n=10) that was set at 100% of germination. Asterisks represent significant differences from Col-0 according to a Student's t test: (*) p≤0.05, (**) p≤0.01 and (***) p≤0.001. (B) Percentage of abnormal pollen tubes over total germinated pollen for simple, double and the triple mutant *lrx9-2 lrx10-1 lrx11-1* after 3 h of germination. Data are shown as the mean ± SEM for Col-0 (n=33), for *lrx8-2* (n=3), for *lrx9-2* (n=4), for *lrx10-1* (n=8), for *lrx11-1* (n=7), for *lrx8-2 lrx10-1* (n=7), for *lrx9-2 lrx11-1* (n=6), for *lrx9-2 lrx10-1* (n=3) and for *lrx9-2 lrx10-1 lrx11-1* (n=15) where "n" corresponds to the number of independent plants with more than 80 pollen grains analyzed per genotype and experiment. Asterisks indicate significant differences from Col-0 according to a one-way ANOVA test: (***) p≤0.001. (C) Representative DIC images of WT and *lrx9-2 lrx10-1 lrx11-1* pollen tubes. Scale bar: 10 µm.

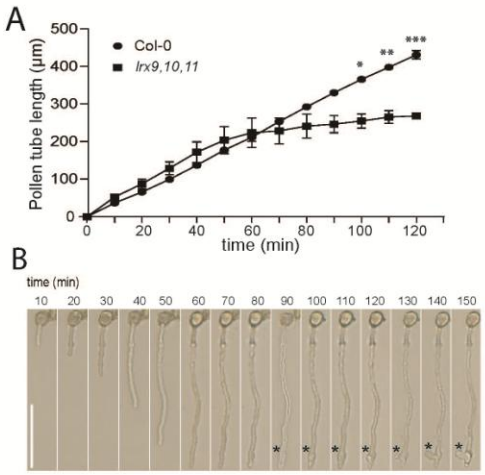

Figure 3 (A) Kinetic analysis of in vitro growing of Col-0 and triple mutant *lrx9-2 lrx10-1 lrx11-1* pollen tubes. Data are shown as the mean ± SEM of two independent experiments with 7 pollen tubes analyzed per experiment. Asterisks indicate significant differences from Col-0 according to Student's t test (*) p≤0.05, (**) p≤0.01 and (***) p≤0.001. **(B)** *In vitro* growing time-lapse image of a representative abnormal pollen tube of the triple mutant *lrx9-2 lrx10-1 lrx11-1*. Asterisks indicate where a bulge is formed. Scale bar=100 µm. Pollen tubes stop growing before forming the bulges at the tip and frequently burst.

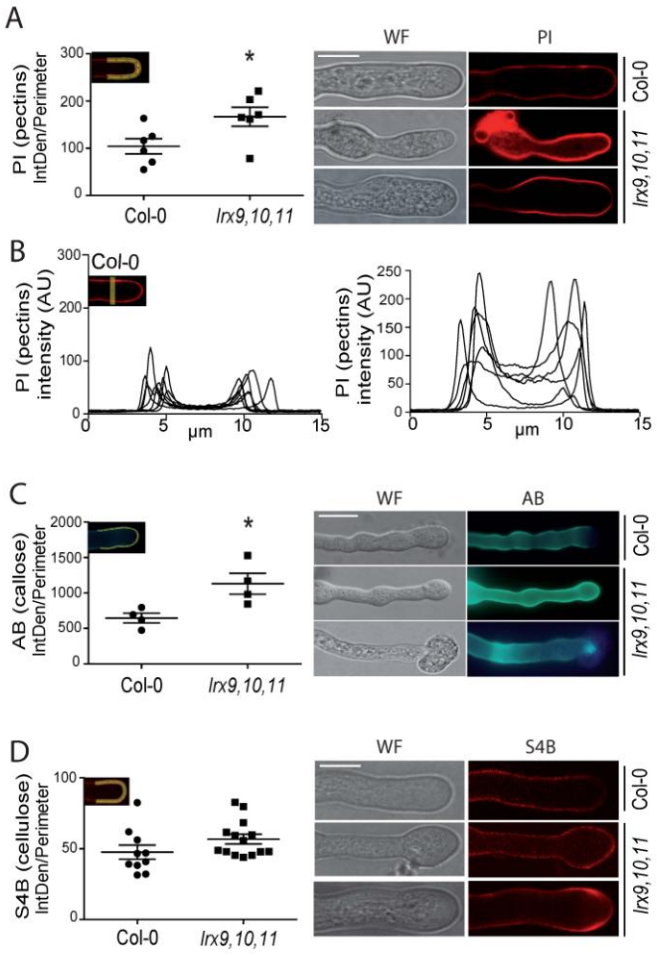

Figure 4 Quantification of cell wall components in Col-0 and triple mutant *lrx9-2 lrx10-1 lrx11-1* pollen tubes. Representative images of pollen tubes stained with propidium iodide (PI) **(A-B)**, aniline blue (AB) **(C)** and Pontamine Fast Scarlet 4B (S4B) **(D)**. Asterisks indicate significant differences from Col-0 according to Student's t test (*) p≤0.05. Scale bar: 5 µm (A); 10 µm (C-D). For PI **(A)**, AB **(C)** and S4B **(D)** quantifications, a signal along the cell wall of the pollen tubes from the tip into the subapical area was obtained. The fluorescent signal was normalized to the pollen tube perimeter of the measured region. For **(B)**, a transversal line at 5 µm away from the tip was defined. Triple mutant measurements were performed including all pollen tubes despite their degree of abnormality; the bulge was always excluded from the measurements.

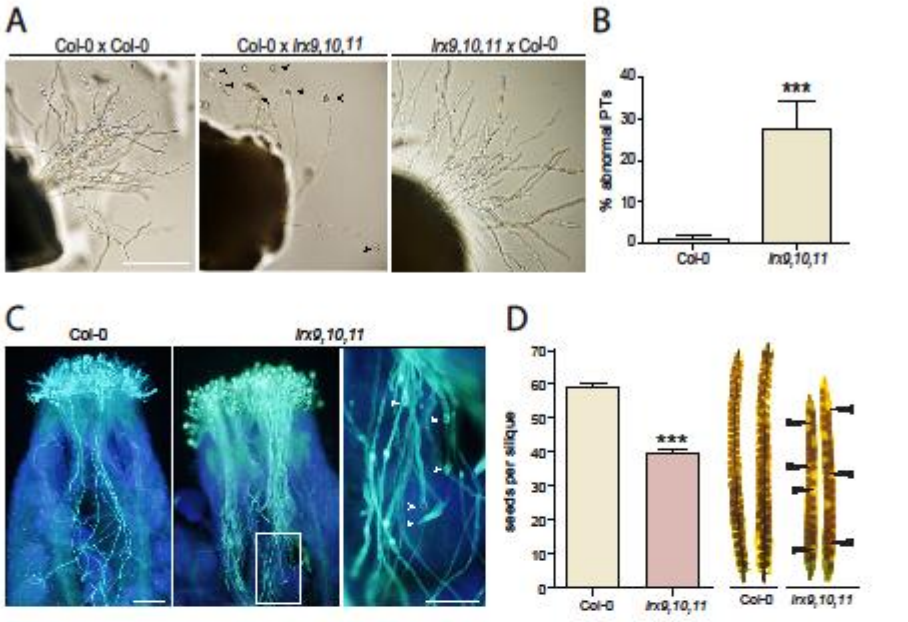

Figure 5 (A) Representative images of WT (left and right panel) and triple mutant *lrx9-2 lrx10-1 lrx11-1* (middle panel) pollen tubes growing through WT (left and middle panels) or triple mutant *lrx9-2 lrx10-1 lrx11-1* (right panel) pistils in a semi *in vivo* assay. Styles were observed 3h after hand pollination. Arrowheads indicate abnormal pollen tubes found only in mutant pollen. Scale bar: 200 µm. (B) Semi-*in vivo* assays quantification. Data are shown as the mean ± SEM of 13 and 8 pollinations for WT and the triple mutant *lrx9-2 lrx10-1 lrx11-1*, respectively. (C) Representative images of aniline blue staining of *in vivo* WT (left panel) and triple mutant *lrx9-2 lrx10-1 lrx11-1* (middle panel) growing pollen tubes 4 h after hand pollination. Left panel shows an inset of the middle image as indicated. Arrowheads indicate abnormal pollen tubes. Scale bars: left and middle panel: 100 µm, right panel: 50 µm. (D) Number of seeds per silique in WT and triple mutant *lrx9-2 lrx10-1 lrx11-1* plants. Data are shown as the mean ± SEM of 11 independent plants with 10 siliques analyzed for each plant. Asterisks indicate significant differences from Col-0 according to a Student's t test with (***) p≤0.001. Arrowheads indicate unfertilized or aborted ovules.